Journal of Solid State Chemistry 246 (2017) 379–387

Contents lists available at ScienceDirect

Journal of Solid State Chemistry

journal homepage: www.elsevier.com/locate/jssc

Solid state synthesis of Mn_5Ge_3 in Ge/Ag/Mn trilayers: Structural and magnetic studies

V.G. Myagkov[a,*], L.E. Bykova[a], A.A. Matsynin[a], M.N. Volochaev[a], V.S. Zhigalov[a], I.A. Tambasov[a], Yu L. Mikhlin[b], D.A. Velikanov[a], G.N. Bondarenko[b]

[a] Kirensky Institute of Physics, SB RAS, Krasnoyarsk 660036, Russia
[b] Institute of Chemistry and Chemical Technology, SB RAS, Krasnoyarsk 660049, Russia

ARTICLE INFO

Keywords:
Long-range atomic transfer
Mn-Ge system
Thin-film solid-state reaction
Diffusion barrier
Dominant diffusing species
First phase
Mn_5Ge_3 alloy

ABSTRACT

The thin-film solid-state reaction between elemental Ge and Mn across chemically inert Ag layers with thicknesses of (0, 0.3, 1 and 2.2 μm) in Ge/Ag/Mn trilayers was studied for the first time. The initial samples were annealed at temperatures between 50 and 500 °C at 50 °C intervals for 1 h. The initiation temperature of the reaction for Ge/Mn (without a Ag barrier layer) was ~ 120 °C and increased slightly up to ~ 250 °C when the Ag barrier layer thickness increased up to 2.2 μm. In spite of the Ag layer, only the ferromagnetic Mn_5Ge_3 compound and the Nowotny phase were observed in the initial stage of the reaction after annealing at 500 °C. The cross-sectional studies show that during Mn_5Ge_3 formation the Ge is the sole diffusing species. The magnetic and cross-sectional transmission electron microscopy (TEM) studies show an almost complete transfer of Ge atoms from the Ge film, via a 2.2 μm Ag barrier layer, into the Mn layer. We attribute the driving force of the long-range transfer to the long-range chemical interactions between reacting Mn and Ge atoms.

1. Introduction

Although thin films have been widely used in advanced electronic devices, the atomic migration during thin-film solid state reactions continues to be the subject of many investigations [1–5]. Numerous studies of solid-state reactions in nanofilms showed that there are three fundamental features that strongly distinguish them from bulk samples:

(i) Formation of only the ***first phase*** at the film interface at a certain temperature T_{in} called the ***initiation (formation) temperature*** T_{in}. As the annealing temperature increases, other phases can occur and form the phase sequence [3–8].
(ii) The threshold of the reaction, characterized by intense intermixing at the interface and the formation of compounds, arises at temperatures above the initiation temperature T_{in} [3–5].
(iii) Migration of the dominant diffusing species through the interface during the first phase formation [5,9,10].

The formation of only the first phase among the equilibrium phases, the low initiation temperatures that can be below room temperature [11,12] or even below 90 K [13–16] and the migration of the dominant diffusing species are unique, unexplained features of solid-state reactions in nanofilms. As discussed above, the initiation temperature T_{in} is the threshold temperature. This means that there is no reaction below T_{in} and the reaction initiates just as the temperature of a sample overcomes T_{in}. The analysis of solid-state thin film reactions for many bilayers showed that the initiation temperatures T_{in} often coincide with the solid-state phase transformation temperatures T_K, including the order-disorder phase transitions [17], eutectoid decompositions [18,19], martensitic transformations [19–24], eutectic reactions [25], the superionic transition [26], and spinodal decomposition [27–29]. The equality $T_{in} = T_K$ indicates the common chemical nature that controls both solid-state transformations and solid-state reactions in thin films.

When atomic mixing and formation of new phases at the interface start above T_{in}, various physical characteristics of the film samples, such as electrical resistance, magnetization, transparence optique, heat release etc., begin to radically change. Therefore, the initiation temperature T_{in} can be found using the dependence of these characteristics on the sample temperature. At high heating rates the measurement of temperature precedes the measurement of reaction characteristics and as a result the measured T_{in} can overestimate the value of the real initiation temperature T_{in}. Therefore low heating rates (< 10 °C/min) are required for finding the exact T_{in} value.

In recent years, characteristics of the ignition and self-propagation of reactions in reactive multilayer films were intensively investigated [1,2]. Above the initiation temperature T_{in}, the reaction starts by

* Corresponding author.

http://dx.doi.org/10.1016/j.jssc.2016.12.010
Received 2 August 2016; Received in revised form 7 December 2016; Accepted 10 December 2016
Available online 12 December 2016

sluggish atomic migration of reagents across the total interface (diffusion regime). At high heating rates, when the rate of heat generation $Q_{reaction}$ overcomes the rate of heat loss Q_{loss} ($Q_{reaction} > Q_{loss}$), the temperature of the multilayer film strongly increases and above the ignition temperature T_{ig} the reaction jumps into a self-propagating mode. Therefore, the initiation temperature T_{in} is always less than the ignition temperature T_{ig} ($T_{in} < T_{ig}$). Recently, Frits et al. showed that, similar to $T_{in,}$ the ignition temperature T_{ig} is a threshold temperature, because in hot plate experiments the multilayers do not ignite when the specimens are heated to temperatures just 1 °C below T_{ig} [30].

The ferromagnetic Mn_5Ge_3 phase is the first phase which arises at the non-ferromagnetic Ge/Mn interface above the initiation temperature T_{in} ~ 120 °C. The Mn_5Ge_3 phase has been widely investigated as a promising compound for spintronic devices as it has a Curie temperature above room temperature (T_C=304 K), sufficiently high spin polarization (P=42 ± 5%) and it grows on Ge(111) and Ge(001) substrates by solid phase epitaxy [31–38]. The Mn_5Ge_3 phase also forms during low-temperature (~120 °C) spinodal decomposition and this can explain the ferromagnetic formation in Mn_xGe_{1-x} dilute semiconductors [39–45]. Recently we have shown that the initiation temperature T_{in}(Ge/Mn) in Ge/Mn bilayers coincides with the spinodal decomposition temperature T_K=120 °C of a solid solution in the Ge-Mn system [28,29]. This clearly demonstrates that the same chemical interactions underlie both the solid state reactions in Ge/Mn bilayers and spinodal decomposition in the Ge-Mn system.

We deposited chemically inert silver layers (diffusion barriers) of different thicknesses between the Ge and Mn films to investigate the features of the Mn_5Ge_3 synthesis. However, only results for thicknesses of 0, 0.3, 1 and 2.2 μm for the Ag layer are presented in the paper. Silver was chosen as the interlayer material because it does not react chemically with Ge and Mn and does not form stable phases with these elements. According to the phase equilibrium diagrams, Ag does not mix with Ge up to the eutectic temperature 651 °C [46]. The experimental data reported confirms the absence of mixing on the Ag/Ge(111) interfaces up to 660 °C [47]. The Mn/Ag superlattices with a Ag buffer layer (~2.2 nm) show very sharp interfaces [48]. Our cross-sectional TEM studies show that annealing treatments for 1 h at 300 °C and 500 °C corroborate the lack of significant mixing at the Ag/Ge and Ag/Mn interfaces. Therefore the formation started in the nonmagnetic Ge/Mn and Ge/Ag/Mn films with annealing temperatures above the initiation temperature T_{in} ~120 °C of the ferromagnetic phase, having a Curie temperature T_C ~304 K are associated only with Mn_5Ge_3 synthesis.

In this article, we report a systematic study of the migration of Ge atoms, via chemically inert Ag barriers of thicknesses 0, 0.3, 1 and 2.2 μm, to a Mn layer for the formation of the Mn_5Ge_3 phase. Basic findings consist of the appearance of strong long-range chemical interactions above the initiation temperature T_{in} ~ 120 °C, at which the synthesis of the Mn_5Ge_3 phase starts even if the reacting Mn and Ge atoms are separated by a distance about 10^4 greater than an ordinary chemical bond length.

2. Experimental details

2.1. Sample preparation

The initial Ge/Ag/Mn and Mn/Ag/Ge films were obtained by the successive thermal deposition of Mn, Ag, Ge, and Ge, Ag, Mn, layers, respectively, onto Si(001) and chemically pure glass substrates having a thickness of 0.18 mm in a vacuum at a residual pressure of 10^{-6} Torr. The thicknesses of the chemically inert Ag barrier layers were 0.3 μm for Ge/Ag/Mn (hereafter, Ge/0.3 μm Ag/Mn) and 1, 2.2 μm for Mn/Ag/Ge (hereafter, Mn/1μmAg/Ge and Mn/2.2μmAg/Ge, respectively). For comparison, we analyzed a reference sample of Ge/Mn without the interlayer. Previously, the substrates were degassed at 350 °C for 1 h. All layers except the top layer are deposited at 250 °C. The top layer deposited at room temperature to avoid solid-state reactions between Mn and Ge during deposition. In the experiments we used samples with an approximate 0.6Mn:0.4Ge stoichiometry and a total thickness of ~ 400 nm. Films 0.2μmMn/0.4μmAg/0.2μmGe were obtained for visual observation of the reaction. Film thicknesses were determined by X-ray fluorescent analysis or cross-sectional transmission electron microscopy (TEM) image.

2.2. Synthesis

The initial Ge/Mn bilayers and Ge/0.3μmAg/Mn, Mn/1μmAg/Ge, Mn/2.2 μm Ag/Ge trilayers were annealed at temperatures between 50 and 500 °C at 50 °C intervals. The samples were held at each temperature at a pressure of 10^{-6} Torr for 1 h.

2.3. TEM characterization

The cross-sectional samples for investigation by TEM were prepared using a focused ion beam (FIB, Hitachi FB2100) at 40 kV to a thickness of about 70–80 nm. The samples on Si(001) substrates were prepared by single beam FIB because they possess less accumulation of charge than glass substrates and have low beam drift during preparation.

In order to protect the surface of interest from milling by the Ga+ ion beam during sample preparation, a W layer was deposited in the FIB by dissolution of the $W(CO)_6$ gas. TEM investigations were carried out using a Hitachi HT7700 TEM at 100 kV (W source) equipped with a scanning TEM system and a Bruker Nano XFlash 6T/60 energy dispersive X-ray (EDX) spectrometer. The imaging and EDX spectroscopy line scans and mapping were carried out in scanning TEM mode with an electron probe of diameter ~ 30 nm.

2.4. XPS studies

X-ray photoelectron spectra were collected using a SPECS instrument (Germany) equipped with a PHOIBOS 150 MCD 9 hemispherical analyzer at a pass energy of 20 eV for survey spectra and 8 eV for narrow scans. The Mg K_α line (1253.6 eV) of a dual anode X-ray source was used for excitation. Sample etching with Ar^+ ions was performed with a PU-IQE 12/38 scanning source operated at an accelerating voltage of 5 kV and ion emission current of 15 μA, which correspond to a scattering rate of ~1 nm/min. Relative concentrations of elements were determined from the survey spectra using empirical sensitivity coefficient. The high-resolution spectra were fitted with Gaussian-Lorentzian peak profiles after Shirley background subtraction.

2.5. Magnetic measurements

Saturation magnetization M_S and Curie temperature T_C measurements were performed using superconducting quantum interference device (SQUID) magnetometer in-plane magnetic fields H =0.5 kOe. We also measured the saturation magnetization M_S and the perpendicular anisotropy constant $K_\perp = 2\pi M_S^2 \pm \Delta K_\perp$ using a torque magnetometer with a sensitivity of $3.76 \cdot 10^{-9}$ Nm in the applied field range of 0–18 kOe at room temperature. The value of $\Delta K_\perp$ in thin films was associated with the presence of in-plane strains and the grain growth textures [49,50].

3. Results

3.1. Magnetization measurements

Fig. 1 shows the change of the saturation magnetizations M_S of Ge/Mn (without barrier Ag layer) and Ge/0.3μmAg/Mn, Ge/1μmAg/Mn, Ge/2.2μmAg/Mn films as a function of the annealing temperature. The

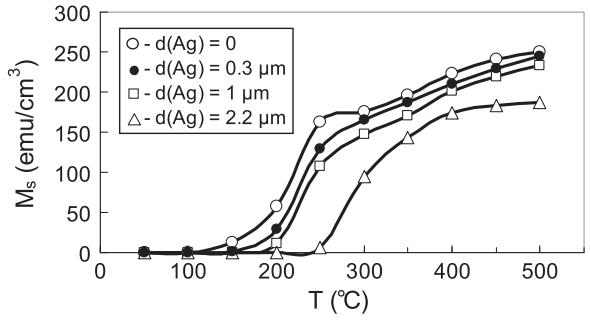

Fig. 1. Temperature dependence of the saturation magnetizations of Ge/Mn and Ge/0.3μmAg/Mn, Ge/1μmAg/Mn, Ge/2.2μmAg/Mn films. All non-ferromagnetic Ge/Mn, Ge/0.3μmAg/Mn, Ge/1μmAg/Mn and Ge/2.2μmAg/Mn samples after annealing above initiation temperatures $T_{in}^{Ge/Mn}$ ~ 120 °C, $T_{in}^{Ge/0.3\mu mAg/Mn}$ ~ 150 °C, $T_{in}^{Ge/1\mu mAg/Mn}$ ~ 200 °C and $T_{in}^{Ge/2.2\mu mAg/Mn}$ ~ 250 °C possess saturation magnetizations which grow with increasing annealing temperatures. These results have clearly demonstrated the low-temperature reaction between Ge and Mn across the Ag buffer layer up to 2.2 μm and the synthesis of the ferromagnetic Mn_5Ge_3.

initial Ge/Mn bilayer and Ge/0.3 μm/Ag/Mn, Ge/1μmAg/Mn and Ge/2.2μmAg/Mn trilayers remain nonmagnetic up to annealing temperatures of ~120 °C, ~150 °C, ~200 °C and ~250 °C, respectively. In all samples the magnetization strongly grows above the initiation temperatures $T_{in}^{Ge/Mn}$ ~ 120 °C, $T_{in}^{Ge/0.3\mu m\ Ag/Mn}$ ~ 150 °C, $T_{in}^{Ge/1\mu mAg/Mn}$ ~ 200 °C, $T_{in}^{Ge/2.2\mu mAg/Mn}$ ~ 250 °C and this clearly demonstrates the onset of intense intermixing of the Ge and Mn atoms and the formation of ferromagnetic Mn_5Ge_3.

3.2. Solid state synthesis of Mn_5Ge_3 in the Ge/Mn bilayers

The X-ray diffraction (XRD) patterns of the initial Ge/Mn bilayers contained α-Mn reflections (Fig. 2a). The absence of Ge reflections suggests that the top Ge layer grew with fine grains. In Ge/Mn bilayers the synthesis of the ferromagnetic Mn_5Ge_3 phase starts above $T_{in}^{Ge/Mn}$ ~ 120 °C and is evident in XRD patterns (Fig. 2a) and magnetic measurements (Fig. 1). The annealing temperature dependence of the magnetization of the Ge/Mn bilayer contains bending (Fig. 1), which is associated with the Mn_5Ge_3 finish at ~ 300 °C [28,29]. Further evidence for the existence of the Mn_5Ge_3 phase after annealing at 300 °C is provided by temperature dependence of the saturation magnetization shown in Fig. 2b, which indicates the formation of the Mn_5Ge_3 phase with a Curie temperature T_C^1 ~ 300 K and a second phase with T_C^2 ~ 400 K (Fig. 2b). Fig. 2b shows that, after annealing at 500 °C, the phase with T_C^2 ~ 400 K had a saturation magnetization M_S ~ 250 emu/cc at room temperature and reflections of the Mn_5Ge_3 phase. Recently, we reported that annealing 60Mn/40Ge and 80Mn/20Ge bilayers above 300 °C leads to incorporating C and O impurity atoms into the octahedral interstitial sites of the Mn_5Ge_3 lattice with the formation of the Nowotny phase $Mn_5Ge_3C_xO_y$, which has a saturation magnetization (M_S ~ 180–320 emu/cc) and a Curie temperature T_C ~ 350–360 K [28,29]. It follows that $Mn_5Ge_3C_xO_y$ is the main phase formed in the Ge/Mn bilayer after annealing at 500 °C. However, secondary ferromagnetic phases, such as Ge_2Mn [51], $D0_{22}$-Mn_3Ge [52], hexagonal Mn_3Ge [53], a-Mn structured Mn_3Ge [54], unknown Mn_3Ge [55] and $Ge_{0.7}Mn_{0.3}$ [56] can arise and possess Curie temperatures higher than the T_C of Mn_5Ge_3 and provide a contribution to the overall magnetic moment and Curie temperature of the reaction products. Also, interphase exchange interactions can lead to an increase of the overall T_C, making it higher than the T_C of Mn_5Ge_3 and modifying the temperature dependence of magnetization after annealing at 500 °C (Fig. 2b).

3.3. Solid state synthesis of Mn_5Ge_3 in the Ge/0.3μmAg/Mn trilayer

The TEM image and the compositional profiles in EDX mode for the

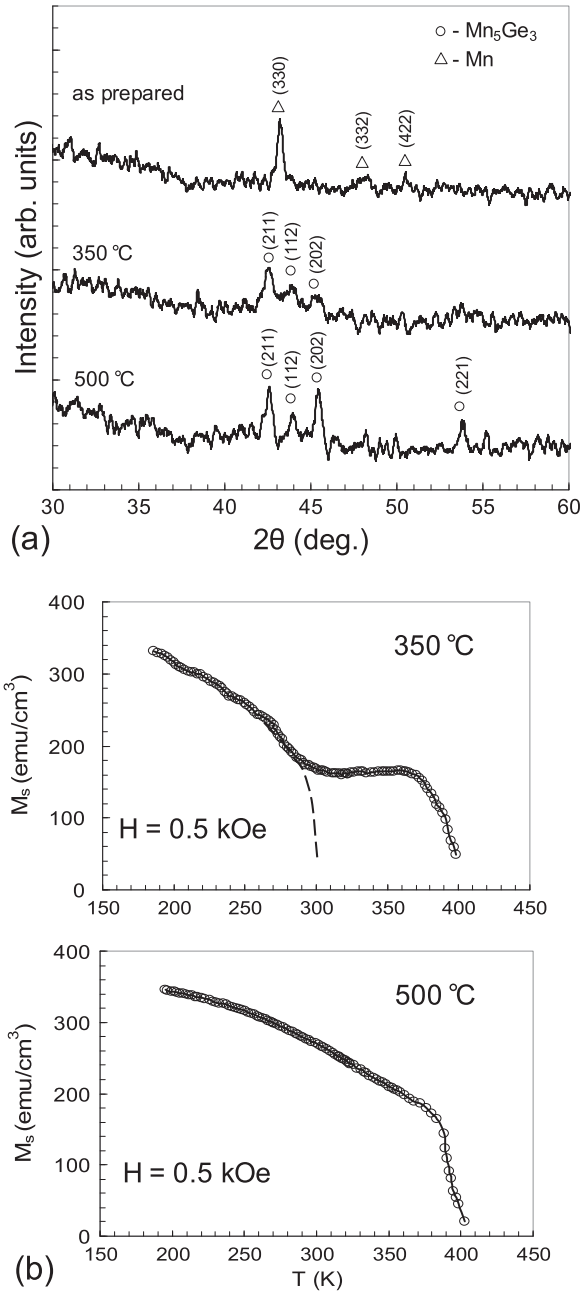

Fig. 2. Characteristics of the Mn_5Ge_3 synthesis in Ge/Mn bilayers. (a) X-ray diffraction patterns of Ge/Mn bilayers in as-prepared and after annealing at 300 °C and 500 °C. (b) Temperature dependence of the saturation magnetization M_S after annealing at 300 °C and 500 °C. The applied in-plane magnetic field was H =0.5 kOe.

initial Ge/0.3μmAg/Mn trilayers have been obtained, and the scanning line is indicated by the solid line in Fig. 3. A trilayer structure which contained the Ge, Ag, and Mn layers is clearly illustrated by TEM and EDX scan results (Fig. 3a) and conform to the XRD data (Fig. 3d). In contrast to the Ge/Mn bilayer, magnetization of the Ge/0.3μmAg/Mn trilayer starts at $T_{in}^{Ge/0.3\mu mAg/Mn}$ ~ 200 °C, sharply grows up to 300 °C and reaches the magnetization magnitude of the Ge/Mn bilayer (Fig. 1). XRD patterns and magnetic measurements unambiguously indicate the formation of Mn_5Ge_3 with T_C ~ 300 K after annealing at 300 °C (Fig. 3d). The TEM image and EDX line scan results of the Ge/0.3μmAg/Mn film after annealing at 300 °C shown in Fig. 3b reliably demonstrates the presence of a considerable quantity of Ge atoms in the Mn layer and this proves that Ge is the dominant diffusing species in the Mn_5Ge_3 synthesis. EDX analysis gives the average value of the

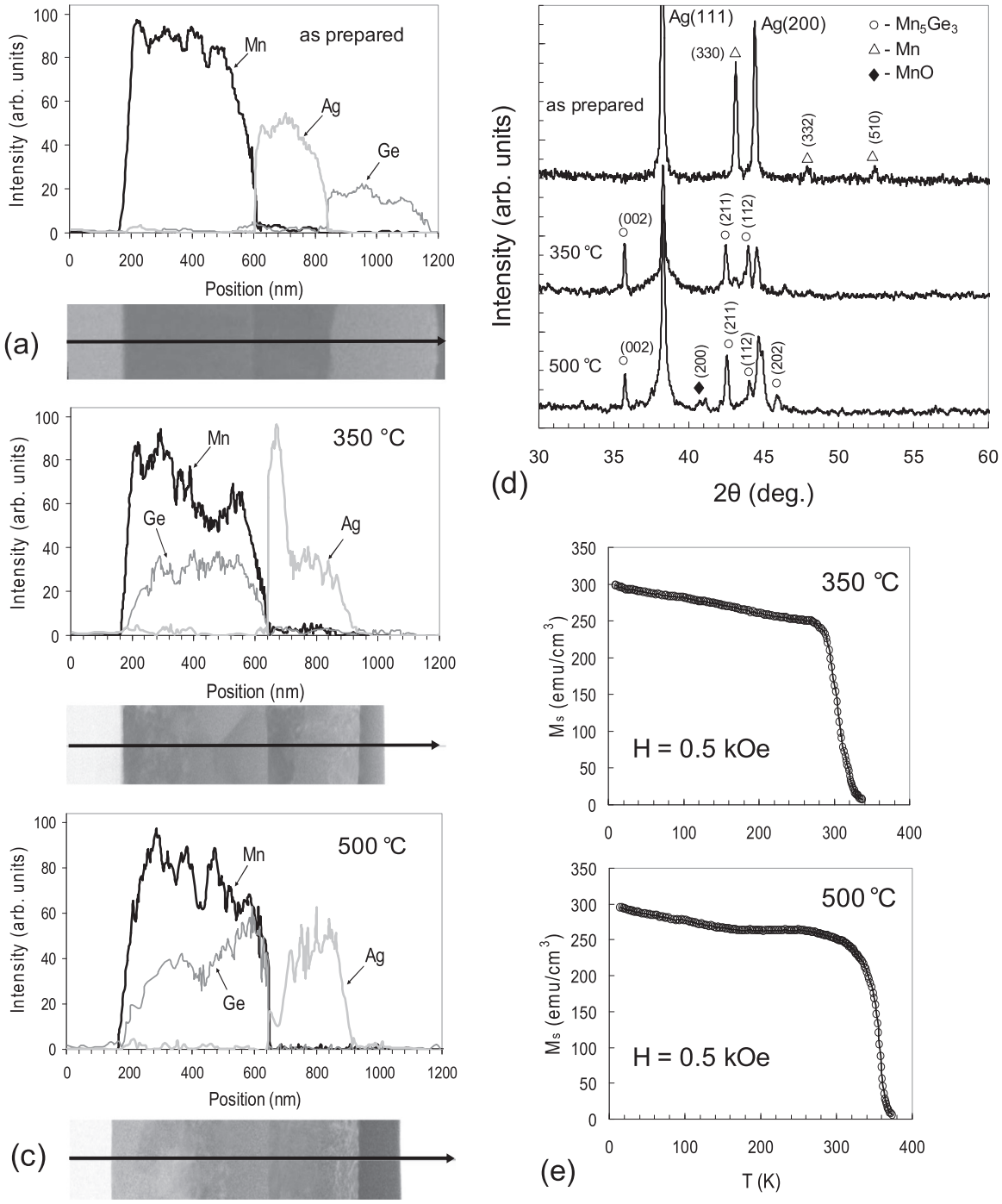

Fig. 3. A direct evidence of the low-temperature synthesis of the Mn_5Ge_3 in Ge/0.3 μmAg/Mn trilayers. TEM image of the cross-section Ge/0.3μmAg/Mn bilayers: (a) as-prepared, (b) after annealing at 350 °C and (c) 500 °C. Compositional profiles of Ag, Ge and Mn of these samples along the scan line shown in the TEM image of the cross-section. (d) X-ray diffraction patterns of Ge/0.3μmAg/Mn trilayers in as-prepared and after annealing at 300 °C and 500 °C. (e) Temperature dependence of the saturation magnetization M_S after annealing at 300 °C and 500 °C. The applied in-plane magnetic field was H =0.5 kOe.

atomic concentration ratio of Mn and Ge near the Mn/Ag interface as about 1.8 which is more than 1.66 for the Mn_5Ge_3 phase. This is strong evidence that even at 500 °C almost all atoms from the Ge film migrated into the Mn film without considerable losses of Ge atoms in the Ag buffer layer and Ge is the sole diffusing species in the Mn_5Ge_3 synthesis (Fig. 3c). Increasing the annealing temperature above 300 °C up to 500 °C did not produce a change in the XRD pattern and it still contained Mn_5Ge_3 peaks (Fig. 3d). The magnetization and Curie temperature increased (Fig. 3e) approximately to the value of the Ge/Mn bilayers (Fig. 1). This is consistent with the results of the Ge/Mn bilayers and suggests the Ge/0.3μmAg/Mn also relates the formation of the Nowotny phase and the secondary ferromagnetic phases to this temperature interval.

3.4. Solid state synthesis of Mn_5Ge_3 in the Ge/2.2 μmAg/Mn trilayer

In a similar way, the 1 μmGe and 2.2 μmGe buffer layers thicknesses did not change the scenario of the synthesis of the Mn_5Ge_3 phase. For the Ge/2.2 μmAg/Mn trilayer XRD pattern of the as-prepared sample contained strong reflections of the Ag layer and a Mn (330) peak and no peaks from the finely-dispersed Ge layer (Fig. 4a). The analysis of the XRD pattern and magnetic measurements

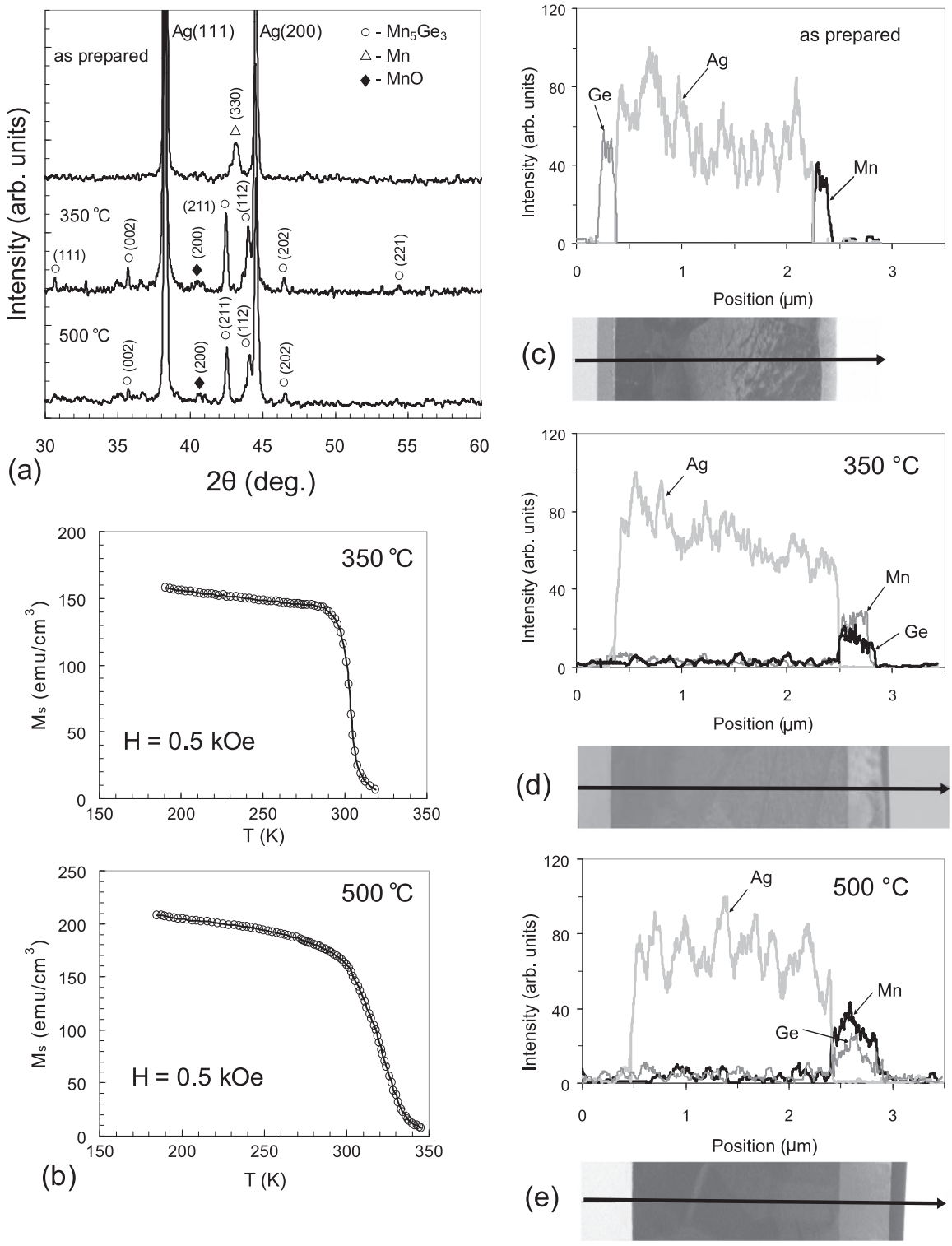

Fig. 4. A direct evidence of the low-temperature synthesis of the Mn_5Ge_3 in Ge/2.2 μmAg/Mn trilayers. (a) X-ray diffraction patterns of Ge/2.2 μmAg/Mn trilayers in as-prepared and after annealing at 300 °C and 500 °C. (b) Temperature dependence of the saturation magnetization M_S after annealing at 300 °C and 500 °C. The applied in-plane magnetic field was H=0.5 kOe. Cross-sectional TEM image of the phase evolution in the Ge/2.2μmAg/Mn trilayers: (c) as-deposited, (d) after annealing at 350 °C and (e) 500 °C. Compositional profiles of Ag, Ge and Mn of these samples along the scan line shown in the TEM image of the cross-section.

show the formation of the Mn_5Ge_3 phase with a Curie temperature T_C ~ 300 K and the Nowotny phase or the secondary ferromagnetic phases with T_C ~ 350 K after annealing at 300 °C and 500 °C, respectively (Fig. 4b). Like the samples with 0.3 μm Ag and 1 μm Ag buffer layer thicknesses the TEM image and the compositional profiles in EDX mode of as-prepared Ge/2.2μmAg/Mn films contained the trilayer Ge/Ag/Mn structure (Fig. 4c) and after annealing at 300 °C and 500 °C show that Ge is the sole dominant diffusion species and form the Mn_5Ge_3 phase at the Ag/Mn interface (Fig. 4d,e). An important point is that after annealing at 300 °C and 500 °C the intensity and full-width at half-maximum of Ag peaks were practically unchanged. This clearly demonstrates that the migration of Ge does not alter the structure of the Ag layer. Since the saturation magnetization of the Ge/2.2 μmAg/Mn trilayer versus annealing temperatures is smaller than that of the

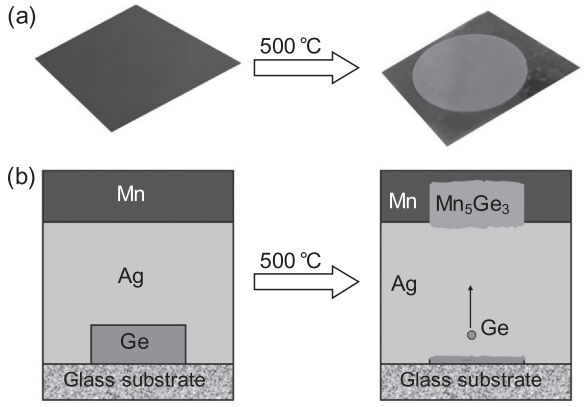

Fig. 5. The direct visualization of the solid state reaction between Mn and Ge across a Ag buffer layer. (a) Photo of the top of the Mn surface of the 0.2 μmMn/0.4 μmAg/0.2 μmGe trilayer before and after annealing at 500 °C. (b) Schematic illustration of the synthesis of $Mn_5Ge_3O_y$ at the Mn/Ag interface by the migration of Ge atoms from the bottom Ge layer across the Ag barrier into the top Mn layer.

Ge/Mn bilayer (Fig. 1), this suggests insignificant losses of Ge atoms in the Ag buffer layer. For all samples the saturation magnetization measurements by the torque method show a very low additional part of the perpendicular anisotropy $\Delta K_{\perp} \sim 0$. These points assume to an absence of the growth texture and in-plane strains in the synthesized Mn_5Ge_3 layers.

3.5. Synthesis imaging

Reactions between Mn and Ge via a Ag buffer layer can be seen by the naked eye. For this purpose a 0.2 μm-Ge layer having the form of a disk is prepared on the glass substrate. After that the 0.4 μm Ag and 0.2 μm Mn layers were sequentially deposited. Fig. 5a shows the modification of the visual image of the upper Mn surface and, on the basis of XPS studies, Fig. 5b represents a schematic illustration of the synthesis of $Mn_5Ge_3O_y$ in the Mn/0.4 μmAg/Mn trilayer after annealing at 500 °C. We investigated the composition and chemical states of Mn, Ge, Ag, and O over the depth (~ 200 nm) of the top part of the 0.2 μmMn/0.4 μmAg /0.2 μmGe sample that was observed on the visual image of the Mn_5Ge_3 layer after annealing at 500 °C (Fig. 5). Fig. 6 presents (a) the X-ray photoelectron spectrum, (b) the relative concentrations of the elements as functions of sputtering time and core-level spectra of the 0.2 μmMn/0.4 μmAg/0.2 μmGe sample after annealing at 500 °C. After eliminating the oxidized and contaminated surface layer, the distribution of Mn and O is almost homogeneous, at least to a depth of 50–60 nm (Fig. 6b). The elemental spectra also change significantly with depth. Below 50–60 nm thickness the X-ray photoelectron spectrum contains Ge, Ag, Mn and O lines and the concentrations of Ge and Ag elements increase with depth up to 120–150 nm (Fig. 6b).

The main contributor to the Mn 2p spectra is the broadband of the multiplet structure typical of MnO (Fig. 6c). This is confirmed by the atomic ratio of Mn/O, which is close to unity, and by the oxygen spectrum with a main line near 530.3 eV (Fig. 6d). In the manganese spectrum, there is also a component (or components) with a binding energy of 639–640 eV that can be attributed to germanides (Fig. 6c). In the Ge 3d spectrum (the Ge 3d core level), the line with a binding energy of 29.4 eV corresponds to the manganese germanide (Fig. 6e). The Mn/Ge ratio of the corresponding lines with binding energies of 640 and 29.4 eV is approximately 4.0, which is higher than that of the Mn_5Ge_3 compound (1.67). This is apparently explained by the presence of the manganese oxide MnO and the Nowotny $Mn_5Ge_3O_y$ phase. In the silver spectrum, the component with a binding energy of 368.3 eV can be attributed to the metallic silver Ag (Fig. 6f).

As noted above, the Ge migration does not alter the structure of the barrier Ag layer, which implies the absence of bulk diffusion and suggests Ge transport along the grain boundaries, dislocations, or pinholes. It is known that the formation of pinholes (ranging up to 150 nm) is a result of rapid atomic diffusion during solid-state reactions [50–52]. Therefore it is reasonable to suggest that pinholes (density of pinholes $> 10^5$ cm^{-2}) are the basic tracks of Ge migration via the Ag barrier layer into the Mn layer. As a result, the rapid Ge migration can induce sizeable interface roughness in pinhole regions without changing the surface relief between pinholes and take Ag atoms with the Ge into the Mn layer. This reaction mechanism can explain the contradiction between the XPS and TEM results. The TEM results between pinholes show Mn/Ag and Ag/Ge interfaces with width up to 50 nm during the migration of Ge atoms into the Mn layer via the Ag barrier layer (Fig. 3a,b,c, Fig. 4c,d,e). However, the main factor that increases the interface width is the atomic mixing obtained by ion beam etching while preparing the cross section samples rather than by the interface reactions. Since the size of the analysis area in XPS is much larger than in TEM, it includes a considerable number of pinholes, and therefore the XPS data shows the presence of silver within the $Mn_5Ge_3O_y$ layer (Fig. 6b).

In summary, the 0.2 μmMn/0.4 μmAg/0.2 μmGe sample, after annealing at 500 °C, contains the top MnO(50–60 nm) layer and the Nowotny $Mn_5Ge_3O_y$ (120–150 nm) phase at the Mn/Ag interface. This result explains the visualization of the $Mn_5Ge_3O_y$ layer via the top (50–60 nm)-MnO layer in the 0.2μmMn/0.4μmAg/0.2μmGe sample after annealing at 500 °C (Fig. 5).

4. Discussion

As discussed above, the Mn-Ge phase diagram, without Mn_5Ge_3, contains many ferromagnetic compounds that are stable at room temperature [54–59]. For all thicknesses (0, 0.3, 1, 2.2 μm) of the Ag layer used in this study, as the annealing temperature increased, only the Mn_5Ge_3 intermetallic compound was observed during the initial stage of the reaction and other phases were not detected. This clearly demonstrates that the formation of the first Mn_5Ge_3 phase in the Ge/Ag/Mn trilayers is independent of the distance between the Ge and Mn reacting layers up to 2,2 μm and only depends on the temperature, which must be above the initiation temperature $T_{in} \sim 120$ °C.

The TEM image and the compositional profiles in EDX mode of as-prepared Ge/2.2μmAg/Mn films after annealing at 300 °C show that Ge is the sole diffusing species. This demonstrates the dominating Ge atomic transfer across the buffer Ag layer into the Mn layer and the formation of the Mn_5Ge_3 phase at the Ag/Mn interface. An important point is that the low initiation temperature T_{in} ~120 °C between Mn and Ge only insignificantly increases up to T_{in} ~250 °C with the increasing of the buffer Ag layer thickness up to 2.2 μm. This difference may be the result of a small annealing time, which was only 1 h hour in our experiments. At such low temperatures, the diffusion coefficients in metal have very low experimental values and therefore they have not yet been identified. This assumes the non-diffusion nature of the atomic transfer of Ge atoms across a buffer Ag layers and is in line with our previous studies, which indicate the exceptional role of long-range chemical interactions during thin-film solid-state reactions [60–64]. Previously, we showed that 2.3 μm-Ag and 1 μm-Ag buffer layers do not prevent thin-film reactions of Pd with Fe and Ni with Fe, respectively [60,61]. In addition, we have reported the solid-state synthesis of the CuAuI ordered phase in epitaxial Au/Co(001)/Cu(001) trilayers where Au and Cu atoms react via inert 2.5 μm-Co(001) layers [62]. Therewith, inert 2.5 μm-Fe and 0.85 μm-Fe layers do not prevent low-temperature reactions of Cd with Au (T_{in} =120 °C) [63] and Cu with β-CuZn (T_{in} =250 °C) [64], respectively.

On the basis of these results, we propose the hypothesized scenario for the synthesis of the Mn_5Ge_3 compound in Mn/2.2 μmAg/Ge trilayers. Above the initiation temperature $T_{in} \sim 120$ °C, strong chemical interactions arise between Mn and Ge atoms for the forma-

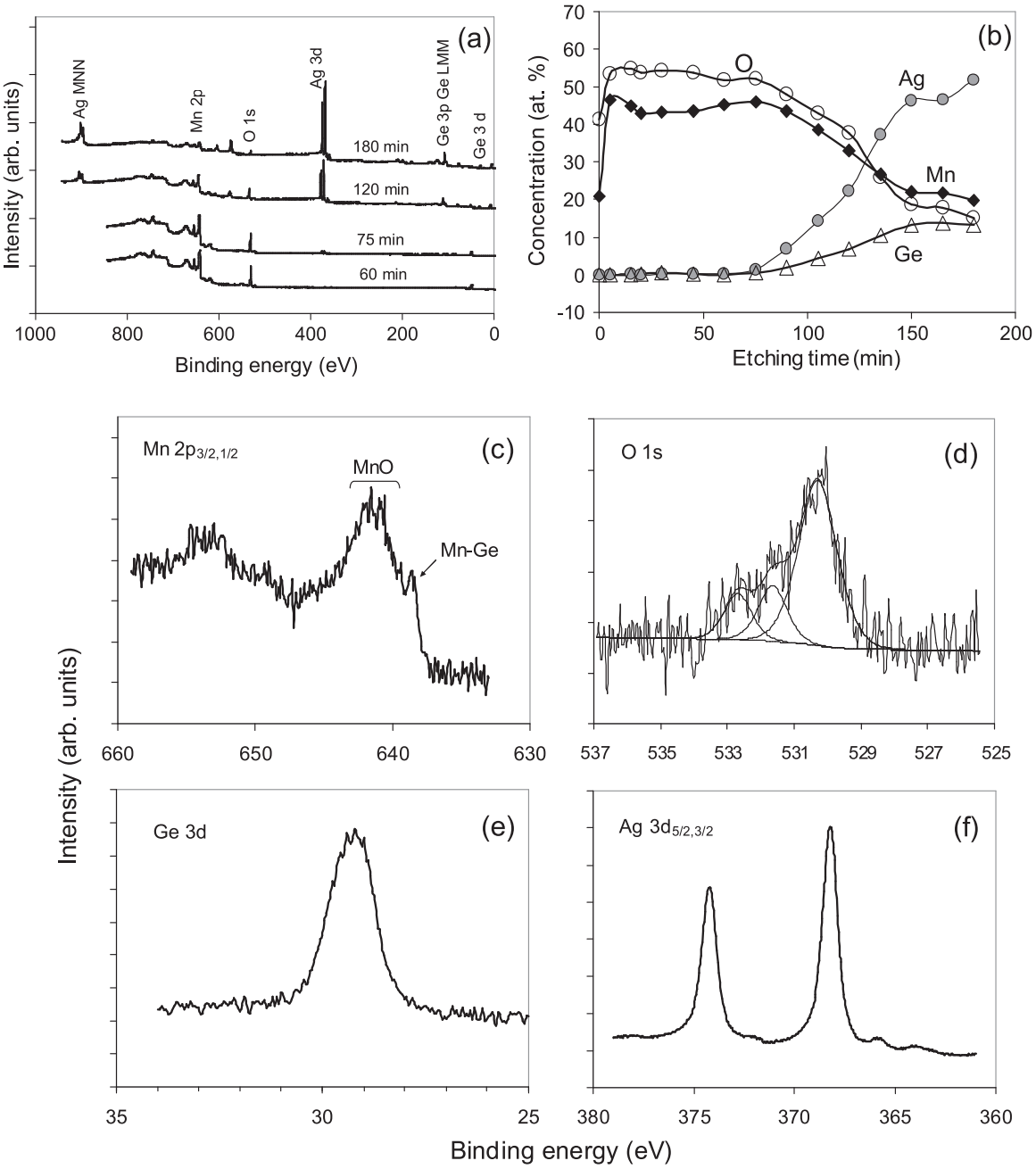

Fig. 6. The XPS date for 0.2 μmMn/0.4 μmAg/0.2 μmGe sample after annealing at 500 °C and Ar^+ sputtering for 180 min (a) XPS spectra, (b) and XPS depth profiles, (c) Mn 2p, (d) O 1s, (e) Ge 3d, (f) Ag 3d spectra.

tion of the Mn_5Ge_3 phase. These interactions break the weak chemical bonds in the Ge layer, generate directional transfer of Ge atoms via a chemically inert Ag layer into the Mn layer and form the Mn_5Ge_3 layer at the Ag/Mn interface. It is significant that magnetic and cross-sectional TEM studies show almost complete transfer of the Ge film via a 2.2 μm Ag layer into the Mn layer, which is not possible for diffusion-controlled reactions. In this study, a Ag layer with thickness up to 2.2 μm was used, but the minimal thickness of the Ag layer which suppresses the reaction between Ge and Mn was not specified. Therefore, the detailed mechanism of long-range reacting atoms transfer requires further investigations.

5. Conclusion

The interfacial reaction between Mn and Ge films starts at ~ 120 °C and the ferromagnetic Mn_5Ge_3 compound forms first in the reaction products. The insertion of chemically inert Ag layers up to 2.2 μm in thickness between the Mn and Ge films doesnot change the synthesis of the Mn_5Ge_3 phase. With increasing thicknesses of the Ag barrier layers up to 2.2 μm, the initiation temperature of the reaction increases up to ~ 250 °C. Cross-sectional studies showed that Ge was the sole diffusing species in Mn_5Ge_3 in all experiments. Analysis of the magnetic and cross-sectional TEM studies show the trivial loss of Ge atoms during their migration from the Ge film via an inert 2.2 μm Ag barrier layer into the Mn layer. Our studies reveal the existence of μm-range atomic transfer of the reacting atoms at low temperatures, at which diffusion is negligible; therefore we propose that the long-range chemical interactions control the atomic transfer, structural rearrangements and synthesis phases in the solid state.

Acknowledgements

This study was supported by the Russian Foundation for Basic Research (RFBR) (Grants # 15-02-00948-a, # 16-03-00069-a), by the Council for Grants of the President of the Russian Federation (SP-1373.2016.3), and by the program of Foundation for Promotion of Small Enterprises in Science and Technology ("UMNIK" program) # 6650GU/2015. The reported study was funded by RFBR and Government of Krasnoyarsk Territory, Krasnoyarsk Region Science and Technology Support Fund to the research project #, 16-42-243006. The XPS and TEM studies were carried out using the facilities of the Performance Service at Krasnoyarsk Scientific Center.

References

[1] T.P. Weihs, Fabrication and characterization of reactive multilayer films and foils,, in: K. Barmak, K.R. Coffey (Eds.), Metallic Films for Electronic, Optical and Magnetic Applications: Structure, Processing and Properties, Woodhead Publishing, Swaston, UK, 2014, pp. 160–243 (Chapter 6).
[2] D.P. Adams, Reactive multilayers fabricated by vapor deposition: a critical review, Thin Solid Films 576 (2015) 98–128.
[3] Thin Films-Interdiffusion and Reaction, in: J.M. Poate, K.N. Tu, J.W. Meyer (Eds.), Willey-Interscience, New York (1978), 1978.
[4] K.N. Tu, J.W. Mayer, L.C. Feldman, Electronic Thin Film Science for Electrical Engineers and Materials Scientists, Macmillan, New York, 1992.
[5] J.E.G. Colgan, A review of thin-film alumitide formation, Mater. Sci. Rep. 5 (1990) 1–44.
[6] R. Pretorius, C.C. Theron, A. Vantomme, J.W. Mayer, Compound phase formation in thin film structures, Crit. Rev. Solid. State Mater. Sci. 24 (1999) 1–62.
[7] T. Laurila, J. Molarius, Reactive phase formation in thin film metal/metal and metal/silicon diffusion couples, Crit. Rev. Solid. State Mater. Sci. 28 (2003) 185–230.
[8] A. Portavoce, G. Tréglia, Physical origin of thickness-controlled sequential phase formation during reactive diffusion: atomistic modeling, Phys. Rev. B 82 (2010) 205431.
[9] M.Y. Tsai, M.H. Chou, C.R. Kao, Interfacial reaction and the dominant diffusing species in Mg–Ni system, J. Alloy. Compd. 471 (2009) 90–92.
[10] C.M. Comrie, D. Smeets, K.J. Pondo, C. van der Walt, J. Demeulemeester, W. Knaepen, C. Detavernier, A. Habanyama, A. Vantomme, Determination of the dominant diffusing species during nickel and palladium germanide formation, Thin Solid Films 526 (2012) 261–268.
[11] V. Simic, Z. Marinkovic, Review room-temperature reactions in thin metal couples, J. Mater. Sci. 33 (1990) 561–624.
[12] R. Juskenas, V. Pakstas, A. Sudavicius, V. Kapočius, V. Karpavičien, Formation of intermetallic phases during ageing of Zn electroplate on the Cu substrate, Appl. Surf. Sci. 229 (2004) 402–408.
[13] M. Seyffert, A. Siber, P. Ziemann, Multiple low-temperature interface reactions: an alternative route into the amorphous state of metallic alloys, Phys. Rev. Lett. 67 (1991) 3792–3795.
[14] H.-G. Boyen, G. Indlekofer, G. Gantner, H. Stupp, A. Cossy-Favre, P. Oelhafen, Intermixing at Au-In interfaces as studied by photoelectron spectroscopy, Phys. Rev. B 51 (1995) 17096–17099.
[15] Th Koch, A. Siber, J. Marien, P. Ziemann, Intermixing at Au-In and Pd-In interfaces at 90 K as observed by in situ Auger-electron and electron-energy-loss spectroscopy, Phys. Rev. B 49 (1994) 1996–2000.
[16] A.Siber, D.Massinger, T.Koch, P.Ziemann, Multilayers - a way to prepare metastable phases by multiple interface reactions, Thin Solid Films 27573-77.s, 1996.
[17] V.G. Myagkov, L.E. Bykova, G.N. Bondarenko, V.S. Zhigalov, A.I. Pol'skii, F.V. Myagkov, Solid-phase reactions, self-propagating high-temperature synthesis, and order-disorder phase transition in thin films, JETP Lett. 71 (2000) 183–186.
[18] V.G. Myagkov, O.A. Baykov, L.E. Bykova, G.N. Bondarenko, The γ-Fe formation in epitaxial Cu(001)/Fe(001) thin films by solid-state synthesis: structural and magnetic features, J. Magn. Magn. Mater. 321 (2009) 2260–2264.
[19] V.G. Myagkov, V.C. Zhigalov, L.E. Bykova, G.N. Bondarenko, Solid-state synthesis and phase transformations in Ni/Fe films: structural and magnetic studies, J. Magn. Magn. Mater. 305 (2006) 534–545.
[20] V.G. Myagkov, Yu.L. Mikhlin, L.E. Bykova, G.V. Bondarenko, G.N. Bondarenko, Long-range nature of chemical interaction in solid-phase reactions: formation of martensite phases of an Au–Cd alloy in Cd/Fe/Au film systems, Dokl. Phys. Chem. 431 (2010) 52–56.
[21] V.G. Myagkov, L.E. Bykova, G.N. Bondarenko, Solid-state synthesis and martensitic transformations in thin films, Dokl. Phys. 48 (2003) 30–33.
[22] V.G. Myagkov, L.E. Bykova, S.M. Zharkov, G.N. Bondarenko, Formation of NiAl shape memory alloy thin films by solid-state reaction, Solid State Phenom. 138 (2008) 377–384.
[23] V.G. Myagkov, V.S. Zhigalov, L.E. Bykova, G.V. Bondarenko, G.N. Bondarenko, Structural and magnetic features of the solid-state synthesis and martensitic transformations in Ni/Fe(001)/MgO(001) thin films, JMMM 310 (2007) 126–130.
[24] V.S. Zhigalov, V.G. Myagkov, O.A. Bayukov, L.E. Bykova, G.N. Bondarenko, A.A. Matsynin, Phase transformations in Mn/Fe(001) films: structural and magnetic investigations, JETP Lett. 89 (2009) 621–625.
[25] V.G. Myagkov, L.E. Bykova, G.N. Bondarenko, Multiple self-propagating high-temperature synthesis and solid-phase reactions in thin films, J. Exp. Theor. Phys. 88 (1999) 963–967.
[26] V.G. Myagkov, L.E. Bykova, G.N. Bondarenko, Superionic transition and self-propagating high-temperature synthesis of copper selenide in thin films, Dokl. Phys. 48 (5) (2003) 206–208.
[27] V.G. Myagkov, L.E. Bykova, G.N. Bondarenko, V.S. Zhigalov, Solid-phase synthesis of solid solutions in Cu/Ni(001) epitaxial nanofilms, JETP Lett. 88 (2008) 515–519.
[28] V.G. Myagkov, V.S. Zhigalov, A.A. Matsynin, L.E. Bykova, G.V. Bondarenko, G.N. Bondarenko, G.S. Patrin, D.A. Velikanov, Phase transformations in the Mn-Ge system and in Ge $_x$ Mn_{1-x} diluted semiconductors, JETP Lett. 96 (2012) 40–43.
[29] V.G. Myagkov, V.S. Zhigalov, A.A. Matsynin, L.E. Bykova, Yu.L. Mikhlin, G.N. Bondarenko, G.S. Patrin, G.Yu Yurkin, Formation of ferromagnetic germanides by solid-state reactions in 20Ge/80Mn films, Thin Solid Films 552 (2014) 86–91.
[30] G.M. Fritz, S.J. Spey Jr., M.D. Grapes, T.P. Weihs, Thresholds for igniting exothermic reactions in Al/Ni multilayers using pulses of electrical, mechanical, and thermal energy, J. Appl. Phys. 113 (2013) 014901.
[31] M. Petit, L. Michez, C.-E. Dutoit, S. Bertaina, V.O. Dolocan, V. Heresanu, M. Stoffel, V. Le Thanh, Very low-temperature epitaxial growth of Mn_5Ge_3 and $Mn_5Ge_3C_{0.2}$ films on Ge(111) using molecular beam epitaxy, Thin Solid Films 589 (2015) 427.
[32] A. Spiesser, H. Saito, R. Jansen, S. Yuasa, K. Ando, Large spin accumulation voltages in epitaxial Mn_5Ge_3 contacts on Ge without an oxide tunnel barrier, Phys. Rev. B 90 (2014) 205213.
[33] D.D. Dung, D. Odkhuu, L.T. Vinh, S.C. Hong, S. Cho, Strain-induced modification in the magnetic properties of Mn_5Ge_3 thin films, J. Appl. Phys. 114 (2013) 073906.
[34] J.H. Grytzelius, H.M. Zhang, L.S.O. Johansson, Surface atomic and electronic structure of Mn_5Ge_3 on Ge(111), Phys. Rev. B 84 (2011) 195306.
[35] W. Ndiaye, M.C. Richter, O. Heckmann, P. De Padova, J.-M. Mariot, A. Stroppa, S. Picozzi, W. Wang, A. Taleb-Ibrahimi, P. Le Fèvre, F. Bertran, C. Cacho, M. Leandersson, T. Balasubramanian, K. Hricovini, Bulk electronic structure of Mn_5Ge_3/Ge(111) films by angle-resolved photoemission spectroscopy, Phys. Rev. B 87 (2013) 165137.
[36] A. Truong, A.O. Watanabe, T. Sekiguchi, P.A. Mortemousque, T. Sato, K. Ando, K.M. Itoh, Evidence of a perpendicular magnetocrystalline anisotropy in a Mn_5Ge_3 epitaxial thin film revealed by ferromagnetic resonance, Phys. Rev. B 90 (2014) 224415.
[37] S.F. Olive Méndez, L.A. Michez, A. Spiesser, V. Le Thanh, Epitaxial growth of strained Mn_5Ge_3 nanoislands on Ge(001), Phys. Status Solidi B 252 (2015) 1854–1859.
[38] V. Le Thanh, A. Spiesser, M.-T. Dau, S.F. Olive-Mendez, L.A. Michez, M. Petit, Epitaxial growth and magnetic properties of Mn_5Ge_3/Ge and $Mn_5Ge_3C_x$/Ge heterostructures for spintronic applications, Adv. Nat. Sci: Nanosci. Nanotechnol. 4 (2013) 043002.
[39] J.-P. Ayoub, L. Favre, I. Berbezier, A. Ronda, L. Morresi, N. Pinto, Morphological and structural evolutions of diluted $Ge_{1-x}Mn_x$ epitaxial films, Appl. Phys. Lett. 91 (2007) 141920.
[40] R.T. Lechner, V. Holý, S. Ahlers, D. Bougeard, J. Stangl, A. Trampert, A. Navarro-Quezada, G. Bauer, Self-assembled Mn_5Ge_3 nanomagnets close to the surface and deep inside a $Ge_{1-x}Mn_x$ epilayer, Appl. Phys. Lett. 95 (2009) 023102.
[41] F. Xiu, Y. Wang, K. Wong, Y. Zhou, X. Kou, J. Zou, K.L. Wang, MnGe magnetic nanocolumns and nanowells, Nanotechnology 21 (2010) 255602.
[42] A. Jain, M. Jamet, A. Barski, T. Devillers, I.-S. Yu, C. Porret, P. Bayle-Guillemaud, V. Favre-Nicolin, S. Gambarelli, V. Maurel, G. Desfonds, J.F. Jacquot, S. Tardif, Structure and magnetism of Ge_3Mn_5 clusters, J. Appl. Phys. 109 (2011) 013911.
[43] E. Biegger, L. Stäheli, M. Fonin, U. Rüdiger, Yu.S. Dedkov, Intrinsic ferromagnetism versus phase segregation in Mn-doped Ge, J. Appl. Phys. 101 (2007) 103912.
[44] S. Yada, P.N. Hai, S. Sugahara, M. Tanaka, Structural and magnetic properties of Ge_{1-x} Mn_x thin films grown on Ge (001) substrates, J. Appl. Phys. 110 (2011) 073903.
[45] B. Toydemir, A.C. Onel, M. Ertas, L.C. Arslan, Dependence of magnetic properties on the growth temperature of Mn0.04Ge0.96 grown on Si (001), J. Magn. Magn. Mater. 374 (2015) 354.
[46] T.B. Massalski, Binary Alloy Phase Diagrams, 2nd ed, ASM International Metals Park, OH, 1990.
[47] C.H. Mullet, S. Chiang, High temperature growth of Ag phases on Ge(111), J. Vac. Sci. Technol. A 31 (2013) 020602.
[48] S. Nahm, L. Salamanca – Riba, B.T. Jonker, G.A. Prinz, A TEM study of epitaxial Fe/Ag and Mn/Ag superlattices, MRS Proc. 160 (1989) 209.
[49] H. Miyajima, K. Sato, T. Mizoguchi, Simple analysis of torque measurement of magnetic thin films, J. Appl. Phys. 47 (1976) 4669–4671.
[50] S. Chikazumi, Epitaxial growth and magnetic properties of single-crystal films of iron, nickel, and permalloy, J. Appl. Phys. 32 (1961) 81S.
[51] M.Liehr, H.Lefakis, F.K.LeGoues, G.W.Rubloff, Influence of thin SiO2 $_{in}$terlayers on chemical reaction and microstructure at the Ni/Si(111) interface, Phys. Rev. B 335517-5525. s, 1986.
[52] L. Ruan, D.M. Chen, Pinhole formation in solid phase epitaxial film of $CoSi_2$ on Si(111), Appl. Phys. Lett. 72 (1998) 3464–3466.
[53] R.T. Tung, Jl Batstone, Control of pinholes in epitaxial $CoSi_2$ layers on Si(111), Appl. Phys. Lett. 52 (1988) 648–650.
[54] M. Jamet, A. Barski, T. Devillers, V. Poydenot, R. Dujardin, P. Bayle-Guillemaud, J. Rothman, E. Bellet-Amalric, A. Marty, J. Cibert, R. Mattana, S. Tatarenko, High-Curie-temperature ferromagnetism in self-organized $Ge_{1-x}Mnx$ nanocolumns, Nat. Mater. 5 (2006) 653–659.
[55] H. Kurt, N. Baadji, K. Rode, M. Venkatesan, P. Stamenov, S. Sanvito, J.M.D. Coey,

Magnetic and electronic properties of $D0_{22}$-Mn_3Ge (001) films, Appl. Phys. Lett. 101 (2012) 132410.
[56] J.F. Qian, A.K. Nayak, G. Kreiner, W. Schnelle, C. Felser, Exchange bias up to room temperature in antiferromagnetic hexagonal Mn_3Ge, J. Phys. D: Appl. Phys. 47 (2014) 305001.
[57] D.D. Dung, W. Feng, Y. Shin, S. Cho, Magnetism and transport properties of α-Mn structure Mn_3Ge thin film, J. Appl. Phys. 109 (2011) 07C310.
[58] T. Matsui, M. Shigematsu, S. Mino, H. Tsuda, H. Mabuchi, K. Morii, Formation of unknown magnetic phase by solid state reaction of thin multilayered films of 75 at% Mn–25 at% Ge, J. Magn. Magn. Mater. 192 (1999) 247.
[59] S.-K. Kim, S. Park, K.J. Yee, J.Y. Son, Y.-H. Shin, M.-H. Jo, T.E. Hong, Electrical and optical observations of ferromagnetism in $Ge_{0.7}Mn_{0.3}$ semiconductor, J. Phys. D: Appl. Phys. 42 (2009) 085005.
[60] V. Myagkov, O. Bayukov, Y. Mikhlin, V. Zhigalov, L. Bykova, G. Bondarenko, Long-range chemical interactions in solid-state reactions: effect of an inert Ag interlayer on the formation of $L1_0$-FePd in epitaxial Pd(001)/Ag(001)/Fe(001) and Fe(001)/Ag(001)/Pd(001) trilayers, Philos. Mag. 94 (23) (2014) 2595–2622.
[61] V.G. Myagkov, V.C. Zhigalov, L.E. Bykova, G.N. Bondarenko, Long-range chemical interaction in solid-state synthesis: chemical interaction between Ni and Fe in epitaxial Ni(001)/Ag(001)/Fe(001) trilayers, Int. J. SHS 18 (2) (2009) 117–124.
[62] V.G. Myagkov, Yu.N. Mikhlin, L.E. Bykova, V.K. Mal'tsev, G.N. Bondarenko, Long-range chemical interaction in solid-state synthesis: the formation of a CuAu alloy in Au/β-Co(001)/Cu(001) epitaxial film structures, JETP Lett. 90 (2009) 111–115.
[63] V.G. Myagkov, Yu.L. Mikhlin, L.E. Bykova, G.V. Bondarenko, G.N. Bondarenko, Long-range nature of chemical interaction in solid-phase reactions: formation of martensite phases of an Au–Cd alloy in Cd/Fe/Au film systems, Dokl. Phys. Chem. 431 (2010) 52–56.
[64] V.G. Myagkov, L.E. Bykova, G.N. Bondarenko, G.V. Bondarenko, Long-range chemical interaction in solid-state synthesis: the Kirkendall effect and solid state reactions in Cu/β-CuZn and Cu/Fe/β-CuZn film systems, JETP Lett. 91 (2010) 665–669.